

# Charge and magnetization inhomogeneities in diluted magnetic semiconductors

Carsten Timm\*

*Institut für Theoretische Physik, Freie Universität Berlin, Arnimallee 14, D-14195 Berlin, Germany*

(Dated: September 26, 2005)

It is predicted that III-V diluted magnetic semiconductors can exhibit inhomogeneous, stripe-like magnetizations and carrier concentrations. This result relies on the strong dependence of the magnetization on the carrier concentration. Within Landau theory a characteristic temperature  $T^*$  below the Curie temperature is found so that below  $T^*$  the equilibrium magnetization shows stripe order. The magnetization modulation is strongly anharmonic. Wavelength and amplitude of the modulation rise for decreasing temperature, starting from zero at  $T^*$ . Above  $T^*$  the equilibrium state is homogeneous but the coupling between charge and magnetization leads to the appearance of an electrically charged layer in domain walls.

PACS numbers: 75.50.Pp, 75.30.Fv, 75.60.Ch, 75.10.Hk

*Introduction.*—Diluted magnetic semiconductors (DMS) are investigated extensively as promising materials for spintronics applications [1, 2] and because of their unique physical properties [3, 4, 5]. Since the magnetic interaction is mediated by carriers, the magnetic properties, such as the magnetization and Curie temperature, depend strongly on the carrier concentration [6, 7, 8, 9, 10, 11]. In fact, the magnetization can be changed *in situ* by tuning the carrier concentration with a gate voltage [6, 7, 9]—a level of control impossible in metals.

Coupling between magnetism and carrier concentration can lead to *inhomogeneous* equilibrium states [12], as found for example in manganites [13], nickelates [14], and cuprates [15]. In DMS, inhomogeneity would appear if the energy gain in regions with higher magnetization and carrier concentration outweighs the loss in exchange energy due to the inhomogeneous magnetization. The present Letter analyzes this possibility for III-V DMS. Lead by the experience with the aforementioned compounds [14, 15, 16, 17], we consider a *stripe-like*, one-dimensional variation of the magnetization. We employ a Landau theory for the coupled magnetic and charge degrees of freedom. This approach is valid on sufficiently long length scales on which the impurity distribution can be treated as homogeneous. One can also expect the coupling to lead to an inhomogeneous charge profile in a domain wall. This question is studied in the final part of this Letter.

*Landau theory.*—The Hamiltonian is written as a functional of the magnetization  $\mathbf{m}$  and the excess carrier density  $\delta n$ . The magnetic part has the usual form

$$H_m = \int d^3r \left\{ \frac{\alpha}{2} m^2 + \frac{\beta}{4} m^4 + \frac{\gamma}{2} \partial_i \mathbf{m} \cdot \partial_i \mathbf{m} \right\}, \quad (1)$$

where  $\partial_i \equiv \partial/\partial r_i$  and summation over  $i$  is implied. The mean-field Curie temperature is determined by  $\alpha = 0$ . Taking its dependence on the carrier concentration into account we expand  $\alpha = \alpha' (T - T_c - \eta \delta n)$ , where  $T_c$  is the Curie temperature for  $\delta n = 0$ . The screened Coulomb energy is

$$H_{\delta n} = \frac{1}{2} \int d^3r d^3r' \frac{e^2}{4\pi\epsilon_0\epsilon} \delta n(\mathbf{r}) \delta n(\mathbf{r}') \frac{e^{-|\mathbf{r}-\mathbf{r}'|/r_0}}{|\mathbf{r}-\mathbf{r}'|}. \quad (2)$$

It is convenient to express  $H_{\delta n}$  in terms of the electrostatic potential  $\phi$ . With  $(\Delta - r_0^{-2})\phi(\mathbf{r}) = -e \delta n(\mathbf{r})/\epsilon_0\epsilon$  (for p-type

DMS) we obtain the total Hamiltonian

$$H = \int d^3r \left\{ \frac{\alpha' (T - T_c)}{2} m^2 + \frac{\beta}{4} m^4 + \frac{\gamma}{2} \partial_i \mathbf{m} \cdot \partial_i \mathbf{m} + \frac{\epsilon_0\epsilon}{2r_0^2} \phi^2 + \frac{\epsilon_0\epsilon}{2} \partial_i \phi \partial_i \phi - \frac{\alpha' \eta \epsilon_0 \epsilon}{2\epsilon r_0^2} m^2 \phi - \frac{\alpha' \eta \epsilon_0 \epsilon}{e} \mathbf{m} \cdot (\partial_i \mathbf{m}) \partial_i \phi \right\}. \quad (3)$$

Equilibrium configurations are given by minima of  $H$  under suitable boundary conditions and subject to the constraint of charge neutrality,  $\int d^3r (\Delta - r_0^{-2})\phi = 0$ , which can be implemented with a Lagrange multiplier. With the averaged squared magnetization  $\overline{m^2}$  and the rescaled potential  $\Phi = (\alpha' \eta \epsilon_0 \epsilon / e) \phi$  the corresponding Euler equations read

$$0 = -a \mathbf{m} \partial_i (\mathbf{m} \cdot \partial_i \mathbf{m}) + b \Delta \mathbf{m} - \underbrace{\left( c + \frac{a}{2r_0^2} \overline{m^2} \right) \mathbf{m}}_{c'} - \underbrace{\left( d - \frac{a}{2r_0^2} \right) m^2 \mathbf{m}}, \quad (4)$$

$$(\Delta - r_0^{-2})\Phi = \frac{a}{2} (\Delta - r_0^{-2})(m^2 - \overline{m^2}) \quad (5)$$

with  $a \equiv \alpha'^2 \eta^2 \epsilon_0 \epsilon / e^2$ ,  $b \equiv \gamma$ ,  $c \equiv \alpha' (T - T_c)$ ,  $d \equiv \beta$ . The only bounded solution of Eq. (5) is  $\Phi = (a/2)(m^2 - \overline{m^2})$ . The equations support the homogeneous mean-field solution  $m^2 = m_0^2 \equiv -c/d > 0$ ,  $\Phi = 0$  for  $T < T_c$ . While Eqs. (4,5) contain five parameters, only two are independent: By suitable rescaling we find  $m(a, b, c, d, r_0; \mathbf{r}) = \sqrt{b}/\sqrt{d} r_0 \hat{m}(a/dr_0^2, cr_0^2/b; \mathbf{r}/r_0)$  and  $\Phi(a, b, c, d, r_0; \mathbf{r}) = b \hat{\Phi}(a/dr_0^2, cr_0^2/b; \mathbf{r}/r_0)$ . Thus it is sufficient to vary two parameters. We choose  $a/dr_0^2 \propto \eta^2$  and  $cr_0^2/b \propto T - T_c$ .

*Periodic solutions.*—We consider solutions of Eqs. (4,5) that are periodic in the  $x$  direction, homogeneous in the  $y$ ,  $z$  directions, and collinear. Equation (4) becomes [18]

$$0 = -a m \partial_x (m \partial_x m) + b \partial_x^2 m - c' m - d' m^3. \quad (6)$$

For a solution with wavelength  $\lambda$ ,  $\overline{m^2} = (1/\lambda) \int_0^\lambda dx m^2(x)$  in  $c'$  turns Eq. (6) into an integro-differential equation. We treat  $c'$  as a parameter, which is then determined selfconsistently. Boundary conditions  $m(0) = m^*$  and  $\partial_x m(0) = 0$  are imposed.  $m^*$  will be obtained by minimizing the energy.

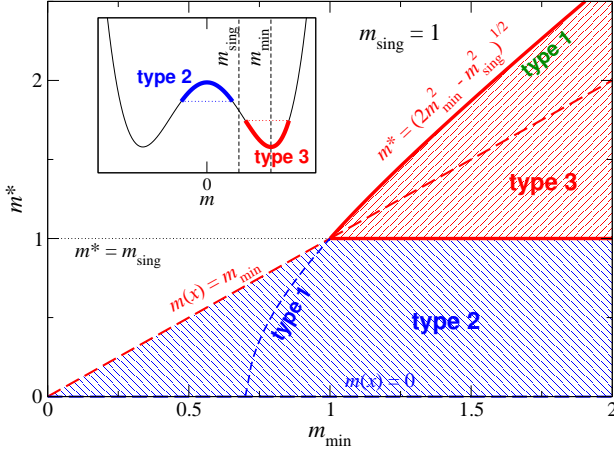


FIG. 1: (color online). Phase diagram for periodic solutions for the magnetization in terms of  $m_{\min}$  and  $m^* = m(0)$  for  $m_{\text{sing}} = 1$ . Type 1 solutions exist for  $m^* = (2m_{\min}^2 - m_{\text{sing}}^2)^{1/2}$  and become a special case of type 2 for  $m^* < m_{\text{sing}}$ . Type 2 solutions exist for  $m^* < \min(m_{\min}, m_{\text{sing}})$  and type 3 solutions for  $m_{\text{sing}} < m^* < (2m_{\min}^2 - m_{\text{sing}}^2)^{1/2}$ . The homogeneous solutions are also shown. Inset: Schematic plot of the denominator in Eq. (7) showing the values assumed by  $m$  for type 2 and 3 solutions.

We now discuss possible periodic solutions. Using standard methods, we obtain the explicit integral for the inverse function on the interval  $[-\lambda/2, \lambda/2]$ ,

$$x = \pm \int_{m^*}^m d\tilde{m} \sqrt{\frac{b - a\tilde{m}^2}{c'\tilde{m}^2 + d'\tilde{m}^4/2 - c'm^{*2} - d'm^{*4}/2}}. \quad (7)$$

This expression satisfies  $\partial_x m(0) = 0$  since  $\partial x / \partial m$  diverges at  $m = m^*$ . To obtain a periodic function, the denominator must have another zero at the next extremum of  $m(x)$  at  $x = \pm\lambda/2$ . Beyond  $\pm\lambda/2$  the solution continues periodically.

A special role is played by the magnetization value  $m_{\text{sing}} \equiv (b/a)^{1/2}$ : If  $m$  reaches  $m_{\text{sing}}$  while the denominator in Eq. (7) remains finite,  $\partial x / \partial m$  vanishes so that coordinates  $x$  beyond this singularity cannot be reached and we do not expect to find a solution for all  $x$ . On the other hand, a solution (here called *type 1*) crossing  $m = m_{\text{sing}}$  is possible if numerator and denominator vanish *simultaneously*. This solution reads  $m(x) = (2m_{\min}^2 - m_{\text{sing}}^2)^{1/2} \cos[(d'/2a)^{1/2}x]$  where  $m_{\min} \equiv (-c'/d')^{1/2}$  is the minimum of the denominator (which is twice the energy density of homogeneous solutions).

For the other periodic solutions the zeros of the denominator are possible extrema of  $m(x)$  and  $m_{\text{sing}}$  must not lie between these extrema. If  $m^* < m_{\text{sing}}$ , real solutions require  $c'\tilde{m}^2 + d'\tilde{m}^4/2 \geq c'm^{*2} + d'm^{*4}/2$ . Periodic solutions (*type 2*) oscillating between  $m^*$  and  $-m^*$  with zero average exist for  $m^* < m_{\min}$ . If  $m^* > m_{\text{sing}}$ , real solutions require  $c'\tilde{m}^2 + d'\tilde{m}^4/2 \leq c'm^{*2} + d'm^{*4}/2$ . Periodic solutions (*type 3*) oscillating around  $m_{\min}$  exist for  $c'm^{*2} + d'm^{*4}/2 < c'm_{\text{sing}}^2 + d'm_{\text{sing}}^4/2$ . The results are summarized in Fig. 1.

Typical solutions of Eq. (6), obtained by numerical inte-

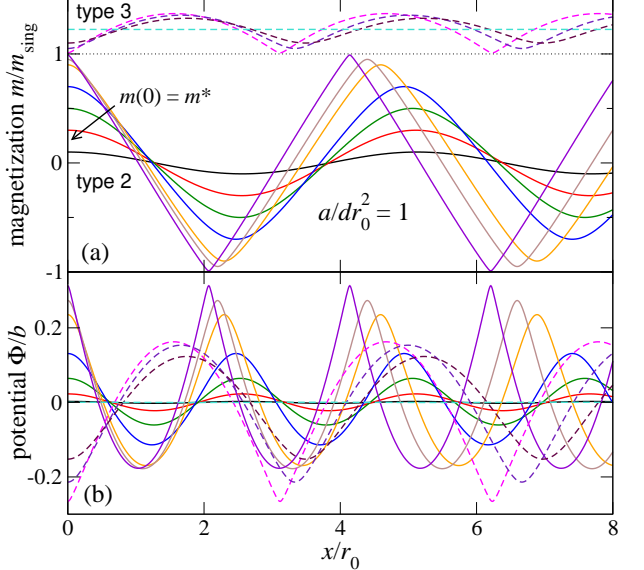


FIG. 2: (color online). (a) Magnetization and (b) electrostatic potential for typical solutions of type 2 (solid curves) and type 3 (dashed curves). One independent parameter is fixed to  $a/dr_0^2 = 1$ . The curves are distinguished by different values of  $m^*/m_{\text{sing}} = 0.1, 0.3, 0.5, 0.7, 0.9, 0.95, 0.99$  (type 2) and  $1.01, 1.05, 1.1, 1.225$  (type 3). Corresponding curves are of the same color.

gration together with iterative adaptation of  $\overline{m^2}$ , are shown in Fig. 2. As  $m^*$  approaches  $m_{\text{sing}}$ , magnetization and potential develop sharp *cusps*. For  $m^* \rightarrow m_{\text{sing}}$  one obtains a solution pieced together from sections of trigonometric functions (but *not* of the type 1 solution since  $\overline{m^2}$  is different). Inspection of Fig. 2(b) shows that the carrier concentration  $\delta n \propto (r_0^{-2} - \Delta)\Phi$  is high where  $m^2$  is large, as expected.

Next, the phase diagram is mapped back onto the parameters of the Euler equation (6), determining  $\overline{m^2}$  selfconsistently. The results are shown in Fig. 3(a) for  $a/dr_0^2 = 1$ . The diagram for other values of  $a$  is topologically identical. To obtain the phase diagram in terms of  $cr_0^2/b$  and *general*  $dr_0^2/a \propto m_{\text{sing}}^2$ , Fig. 3(b), we determine the abscissae of points A, B, C as functions of  $dr_0^2/a$ . In particular, type 3 solutions exist to the left of point A, i.e., for  $m_0 > m_{\text{sing}}$ .

For given parameters, the solution with lowest energy is realized. From Eqs. (3)–(5) we find the average energy density

$$\overline{e} = \frac{1}{\lambda} \int_0^\lambda dx \left\{ -\frac{d'}{4} m^4 + \frac{a}{2} m^2 (\partial_x m)^2 \right\} - \frac{a}{8r_0^2} (\overline{m^2})^2. \quad (8)$$

The energy density of the homogeneous solution is  $e_{\text{hom}} = -c^2/4d$ , as expected. Numerical evaluation shows that type 1 and 2 (type 3) solutions always have higher (lower) energy than the homogeneous solution. Among type 3 solutions the energy is minimized by the maximum amplitude, where  $m$  comes arbitrarily close to  $m_{\text{sing}}$ . In Fig. 2, the curves for  $m^*/m_{\text{sing}} = 1.01$  are thus close to the optimum solution.

The mean-field magnetization of our DMS model is thus

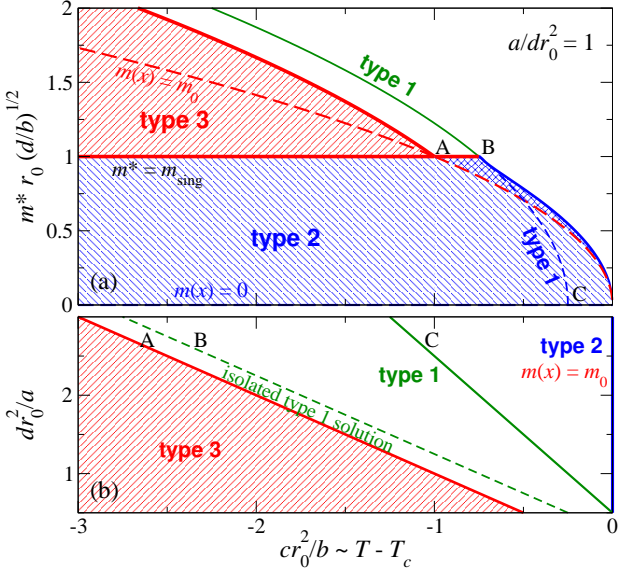


FIG. 3: (color online). (a) Phase diagram for periodic solutions for the magnetization in terms of  $cr_0^2/b \propto T - T_c$  and initial magnetization  $m^* = m(0)$  for  $a/dr_0^2 = 1$ . The symbols are as in Fig. 1. In the distorted triangle with corners A,B,0 two solutions with different wavelength coexist. (b) Phase diagram for periodic magnetization solutions in terms of  $cr_0^2/b \propto T - T_c$  and  $dr_0^2/a \propto m_{\text{sing}}^2$ . The various solutions exist to the left of the respectively lines [18].

zero for  $T \geq T_c$ , homogeneous for  $T^* \leq T < T_c$ , where

$$T^* \equiv T_c - \frac{e^2}{\epsilon_0 \epsilon} \frac{\beta \gamma}{\alpha'^3 \eta^2} \quad (9)$$

corresponds to line A in Fig. 3(b), and a periodic spin-density and charge-density wave for  $T < T^*$ . The dipolar interaction omitted here favors  $\mathbf{m}$  lying in the  $yz$  plane. The magnetization and potential show sharp cusps at the minima of  $m$ . These lead to negative peaks in the carrier density, which become  $\delta$ -functions for  $m^* \rightarrow m_{\text{sing}}$ . This divergence is cut off by the condition that the hole concentration is non-negative. Since the amplitude, wavelength, and energy approach finite values for  $m^* \rightarrow m_{\text{sing}}$ , the Landau theory gives a good impression of the profile, except for some broadening of the cusps.

The optimum solution can be written down explicitly,

$$m(x) = \sqrt{2m_{\text{min}}^2 - m_{\text{sing}}^2} \sin\left(\sqrt{\frac{d'}{2a}} x + \theta\right) \quad (10)$$

for  $0 \leq x \leq \lambda$  and periodically repeated. Here,  $(2m_{\text{min}}^2 - m_{\text{sing}}^2)^{1/2} \sin \theta = m_{\text{sing}}$ . From  $m(x)$  one can obtain expressions for the wavelength  $\lambda = 2(2a/d')^{1/2} (\pi/2 - \theta)$ , the average magnetization  $\bar{m}$ , the peak-to-peak amplitude  $\delta m_{\text{pp}} = (2m_{\text{min}}^2 - m_{\text{sing}}^2)^{1/2} - m_{\text{sing}}$ , and the energy, see Fig. 4.

It is important to check whether the periodic solution can occur in real DMS. Equation (9) shows that  $T_c - T^*$  is small for high dielectric constant, small spin stiffness, strong dependence of  $T_c$  on carrier concentration, and quick onset of magnetization below  $T_c$ . For (Ga,Mn)As we estimate  $T^*$

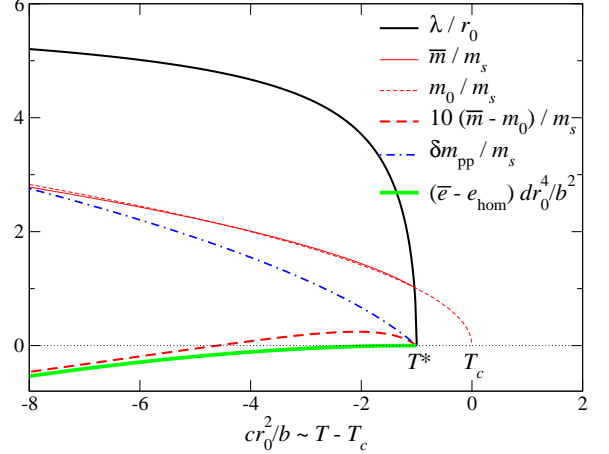


FIG. 4: (color online). Wave length  $\lambda$ , average magnetization  $\bar{m}$ , peak-to-peak amplitude  $\delta m_{\text{pp}}$ , and gain in energy density  $\bar{e} - e_{\text{hom}}$  for the periodic magnetization with lowest energy. The magnetization for the homogeneous solution is also shown. The unit of magnetization is  $m_s \equiv (b/d)^{1/2}/r_0$ .  $a/dr_0^2 = 1$  is assumed.

by comparing experiments [8, 10] to mean-field theory for homogeneous magnetization [19] and to spin-wave theory [20]. We find  $T_c - T^*$  of the order of 10 K. The properties of (Ga,Mn)As vary strongly with Mn concentration and growth and annealing procedures. In particular,  $T_c - T^*$  is inversely proportional to the square of the shift of  $T_c$  with carrier concentration,  $\eta^2$ . In Ref. [10],  $\eta \sim 5.4 \times 10^5 \text{ \AA}^3$ , which was used for the above estimate, whereas in Ref. [8]  $\eta \sim 1.5 \times 10^5 \text{ \AA}^3$ , which would make  $T_c - T^*$  much larger. Figure 4 shows that measurements of the *average* magnetization, which have been performed extensively, are unlikely to find evidence for the inhomogeneous state. The modulation should be observable in neutron-scattering experiments and with magnetic scanning-tunneling microscopy and, for large  $\lambda$ , with magneto-optical techniques.

*Domain walls.*—The Landau theory is now employed to determine the magnetization and potential profile of domain walls. We restrict ourselves to solutions that are homogeneous in the  $y$ ,  $z$  directions. Equations (4,5) are solved under the boundary conditions  $\lim_{x \rightarrow \pm\infty} \mathbf{m}(x) = \pm m_0 \hat{\mathbf{z}}$ , where  $\hat{\mathbf{z}}$  is the unit vector in the  $z$  direction. One can then show that  $\mathbf{m}(x)$  is collinear. Since  $m^2(x)$  only deviates appreciably from  $m_0^2$  in a finite interval, we have  $\bar{m}^2 = m_0^2 = -c/d$  in the limit of infinite system size,  $L \rightarrow \infty$ . However, it turns out that charge neutrality can only be satisfied by keeping terms of order  $1/L$  in  $\bar{m}^2$ . The domain wall contributes one such term and the other comes from the region far from the wall, where we write  $m(L/2) \cong m_0 + m_1/L$ . This means that the enhanced carrier density compensating the reduction in the wall is spread out over the bulk.

With the additional condition  $m(0) = 0$  we obtain

$$x = \int_0^m d\tilde{m} \sqrt{\frac{b - a\tilde{m}^2}{c'\tilde{m}^2 + d'\tilde{m}^4/2 - c'm_0^2 - d'm_0^4/2}} \quad (11)$$

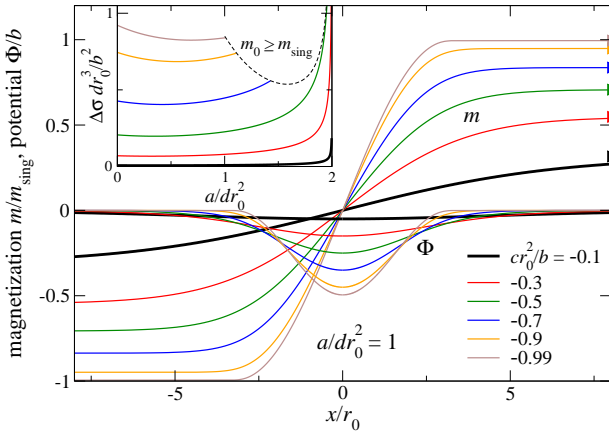


FIG. 5: (color online). Magnetization and electrostatic potential for typical domain-wall solutions for  $a/dr_0^2 = 1$ . The curves are for  $cr_0^2/b = -0.1, -0.3, -0.5, -0.7, -0.9, -0.99$ . The asymptotical values  $m_0 = m(x \rightarrow \infty)$  are indicated by triangles. Inset: Energy density  $\Delta\sigma$  of a domain wall as a function of coupling strength for the same values of  $c$ .

with  $c' = c - (a/2r_0^2)(c/d)$  and  $d' = d - a/2r_0^2$ . The integrand must be real and free of singularities for all  $0 \leq \tilde{m} < m_0$ , which implies  $m_0 \leq m_{\text{sing}}$ . Thus domain-wall solutions only exist for  $T^* \leq T < T_c$  [21]. The boundary condition in the infinite is satisfied since  $x(m)$  diverges for  $m \rightarrow m_0$ .

Equation (11) can be integrated in terms of elementary functions. It also yields an expression for the typical width  $\xi_w \equiv m_0/\partial_x m(0)$  of the domain wall,  $\xi_w^2 = -2bd/c(d - a/2r_0^2)$ .  $\xi_w$  increases for increasing coupling  $a \propto \eta^2$  between magnetism and carriers due to their Coulomb repulsion. Figure 5 shows  $m(x)$  and  $\Phi(x)$  for typical domain-wall solutions. The carrier concentration  $\delta n \propto (r_0^{-2} - \Delta)\Phi$  is reduced in the domain wall, where the magnetization is small.

The areal energy density of the domain wall is obtained by integrating the energy density over  $x$ , where corrections to  $m(x)$  of order  $1/L$  are again relevant in the limit  $L \rightarrow \infty$ ,

$$\Delta\sigma = \int_{-\infty}^{\infty} dx \left[ -\frac{cd}{2(d + a/2r_0^2)} \Delta m^2 - \frac{1}{4} \left( d - \frac{a}{2r_0^2} \right) \times (\Delta m^2)^2 + \frac{a}{8} (\partial_x \Delta m^2)^2 \right] \quad (12)$$

with  $\Delta m^2 \equiv m^2(\pm\infty) - m^2(x)$ . The dependence of  $\Delta\sigma$  on the coupling  $a$  between magnetism and carrier density is shown in the inset of Fig. 5.  $\Delta\sigma$  first decreases with increasing coupling and then increases again, finally diverging as  $d' = d - a/2r_0^2$  goes to zero [18]. For larger  $|cr_0^2/b|$  the divergence is not reached since the condition  $m_0 = m_{\text{sing}}$  (i.e.,  $T = T^*$ ) is satisfied first. The initial decrease is dominated by the  $1/L$  term in  $\Delta m^2(x)$  far from the wall, i.e., from the redistribution of carriers. In this regime, domain walls are less costly and thus more common than they would be without coupling, but the effect is not large. The strong increase mostly comes from the increased wall width due to Coulomb repulsion.

*Conclusions.*—The effects of the carrier-concentration dependence of  $T_c$  in DMS have been investigated. A characteristic temperature  $T^* < T_c$  is found such that the mean-field magnetization  $m$  and excess carrier density  $\delta n$  show periodic modulations for  $T < T^*$ , whereas  $m$  is homogeneous and  $\delta n = 0$  above  $T^*$ .  $T_c - T^*$  can be of the order of 10 K in p-type DMS. The modulation is strongly anharmonic, and amplitude and wavelength increase for decreasing temperature, starting from zero at  $T^*$ . For  $T \geq T^*$  the equilibrium state is homogeneous, but the coupling between magnetism and carrier concentration affects the properties of domain walls. For small coupling the domain-wall energy decreases with increasing coupling. The carrier concentration is reduced in the vicinity of a domain wall, leading to a negatively charged layer (for p-type DMS). This should affect the electronic transport through domain walls [22].

\* Electronic address: timm@physik.fu-berlin.de

- [1] S. A. Wolff *et al.*, Science **294**, 1488 (2001).
- [2] I. Žutić, J. Fabian, and S. Das Sarma, Rev. Mod. Phys. **76**, 323 (2004).
- [3] H. Ohno, Science **281**, 951 (1998); J. Magn. Magn. Mat. **200**, 110 (1999).
- [4] T. Dietl, Semicond. Sci. Technol. **17**, 377 (2002).
- [5] C. Timm, J. Phys.: Cond. Mat. **15**, R1865 (2003).
- [6] H. Ohno *et al.*, Nature (London) **408**, 944 (2000).
- [7] H. Boukari *et al.*, Phys. Rev. Lett. **88**, 207204 (2002).
- [8] K. W. Edmonds *et al.*, Appl. Phys. Lett. **81**, 3010 (2002).
- [9] A. M. Nazmul *et al.*, Jpn. J. Appl. Phys. **43**, L233 (2004).
- [10] X. Liu *et al.*, Phys. Rev. B **71**, 035307 (2005).
- [11] H. Kato *et al.*, Jpn. J. Appl. Phys. **44**, L816 (2005).
- [12] E. Dagotto, Science **309**, 257 (2005).
- [13] M. B. Salamon and M. Jaime, Rev. Mod. Phys. **73**, 583 (2001).
- [14] C. H. Chen, S.-W. Cheong, and A. S. Cooper, Phys. Rev. Lett. **71**, 2461 (1993).
- [15] J. H. Cho, F. C. Chou, and D. C. Johnston, Phys. Rev. Lett. **70**, 222 (1993); J. M. Tranquada *et al.*, Nature (London) **375**, 561 (1995).
- [16] O. Zachar, S. A. Kivelson, and V. J. Emery, Phys. Rev. B **57**, 1422 (1998).
- [17] C. Timm and K. H. Bennemann, J. Low Temp. Phys. **117**, 205 (1999).
- [18] We restrict ourselves to the case  $d' > 0$ , which corresponds to sufficiently weak coupling between magnetization and carrier density. For  $d' < 0$  our Hamiltonian would not be bounded from below so that a  $m^6$  term would be required to stabilize the system. This is expected to lead to a first-order transition.
- [19] J. König *et al.*, in *Electronic Structure and Magnetism of Complex Materials*, Springer Series in Material Sciences **54**, edited by D. J. Singh and D. A. Papaconstantopoulos (Springer, Berlin, 2003), p. 163.
- [20] T. Jungwirth *et al.*, Phys. Rev. B **66**, 012402 (2002).
- [21] If one imposes the same boundary conditions for  $T < T^*$  the solution must cross the singularities at  $\pm m_{\text{sing}}$ . Thus only a type 1 solution is possible. Figure 3(a) shows that its amplitude is larger than  $m_0$  so that it can indeed mediate between  $\pm m_0$ .
- [22] H. Tang and M. L. Roukes, Phys. Rev. B **70**, 205213 (2004).